Turkish J. Eng. Env. Sci.
31 (2007) , 71 – 78.

Intermetallic Phase Formation at Fe-Al Film Interfaces

Güvenç TEMİZEL, Macit ÖZENBAŞ
Department of Metallurgical and Materials Engineering, Middle East Technical University, 06531 Ankara-TURKEY
e-mail: ozenbas@metu.edu.tr

Received 25.08.2006

Abstract

An Fe-Al thin film system was studied for the purpose of examining the formation and development of intermetallic phases, which were formed at the aluminum (Al) film-steel substrate interfaces. Al films having different initial thicknesses in the range of 2μ-14μm were deposited by physical vapor deposition and were then annealed at different temperatures (range: 300-650 °C) and for different time intervals (10 min-8 h). In order to explain the formation mechanisms of the intermetallics at the mentioned Al-Fe film interfaces, X-ray diffractograms (XRD), scanning electron microscopy (SEM), and energy dispersive spectroscopy (EDS) studies were used. The results showed that the intermetallic phases $FeAl_2$ and Fe_2Al_5 were the most dominant phases that could be observed, and that they were formed sequentially, in contrast to intermetallics, which formed synchronously in bulk materials.

Key words: Intermetallics, Fe-Al system, Thin films, Interfaces.

Introduction

Among ordered intermetallics, aluminides possess many attractive properties for structural use at elevated temperatures in harsh environments. These intermetallics have relatively low densities, high melting points, good thermal conductivity, and superb high temperature strength. As a result, these intermetallics are particularly suited for structural applications at elevated temperatures (Wang et al., 1997). They also exhibit many peculiar properties that may find important applications in various fields in the form of thin films. In particular, they show soft magnetic properties, such as low coercivity and high permeability, which make them suitable for thin film-type magnetic heads (Carbucicchio et al., 1999). There is an increasing use of thin films in electronics, either as complete thin film circuits or, more generally, as interconnections and contacts in integrated circuits (Özenbaş and Güler, 2003). Diffusion in thin, vacuum-deposited films is a phenomenon which has received significant attention (Güler, 1997).

The aim of this study was to examine the effect of initial film thickness, and annealing parameters of time and temperature on the formation and development of intermetallic phases at Fe-Al film system interfaces produced by physical vapor deposition (PVD).

Experimental Procedure

Thin film samples of Al on low-carbon steel (ASTM 1112 steel) substrates about 5 × 5 mm^2 were prepared by resistive evaporation of pure Al thin wires. For the deposition of the steel substrates, a vacuum deposition unit (Nanotech Thin Films Ltd., Model Microprep 300-S, Manchester, UK) was used. A tungsten filament was used for vacuum evaporation of Al. The vacuum chamber was pumped out, the evaporant materials being previously placed within. Deposition was started once a pressure of 1×10^{-4} Torr was achieved in order to produce sufficiently fast deposition rates and to help the steel substrate surfaces to outgas (to some extent) without baking them. No substrate heating was applied other than the radiation heat from the source. A horizontal alu-

mina tube furnace equipped with a programmable controller (ABB Kent Taylor-Commander 3000) was utilized in the post-deposition annealing of the films in open alumina crucibles. After deposition of Al films having different initial thicknesses of 2μ, 3μ, 8μ and 14 μm, they were annealed at different temperatures (300, 500, 550, and 650 °C) and for different annealing times (10 min, 30 min, 1 h, 2 h, 3 h, 4 h, 5 h, and 8 h). The heating and cooling rates were set to 10 °C/min and –1.5 °C/min, respectively. The annealing process was carried out under flowing argon.

In this study, the structural properties of the samples were examined by using X-ray diffractogram (XRD), scanning electron microscopy (SEM), and energy dispersive spectroscopy (EDS) analysis. The XRD studies were used to examine the structure of these films. SEM and EDS studies were conducted to investigate the microstructure and the surface morphology of the film samples. X-ray studies were carried out using a Philips Powder Diffractometer in the angle range of 30°-90° with monochromatic CoK_α radiation. Substrate peaks in the diffraction patterns of the samples were determined by using the previously taken patterns belonging to the steel substrate. The samples were further investigated with a Jeol JSM-6400 SEM equipped with an energy dispersive X-ray analyzer. During the SEM and EDS studies, both the film surface and its cross-section were examined. SEM samples were previously coated with a thin (25 nm) layer of gold-palladium alloy to prevent discharging of the specimen during examination.

Results and Discussion

X-Ray Diffraction (XRD) analysis

In Table 1 the intermetallic phases observed according to XRD and EDS analysis are listed along with the experimental conditions of initial thickness, annealing time, and temperature.

By a general approach to Table 1 it could be concluded that the intermetallics $FeAl_2$ and Fe_2Al_5 are the 2 main detectable aluminides. This information is consistent with Table 2, which highlights recent published studies about Fe-Al. In both tables, one or more of the intermetallics ($FeAl_2$, Fe_2Al_5, and $FeAl_3$) were detected using different processing techniques with different annealing cycles.

In Figure 1, X-ray diffractograms are shown for Al films, which were grown on steel substrates and had an initial thickness of 3 μm, that were annealed for 30 min, 1 h, 2 h, 3 h, 4 h, and 5 h at 500 °C, as superimposed on each other to visualize the effect of annealing time on the formation of intermetallics at constant initial thickness and annealing temperature. The intermetallic phase observed first was $FeAl_2$, as can be seen in Figure 1 for 30 min, 1 h, and 2 h. With increased annealing time, Fe_2Al_5 appeared after 3 h. The same results were observed for the films with an initial thickness of 8 μm. The results of X-ray diffractograms of Al films with an initial thickness of 8 μm, which were grown on steel substrates and were annealed for 30 min, 1 h, 2 h, 3 h, 4 h, and 5 h at 500 °C, are shown in Figure 2.

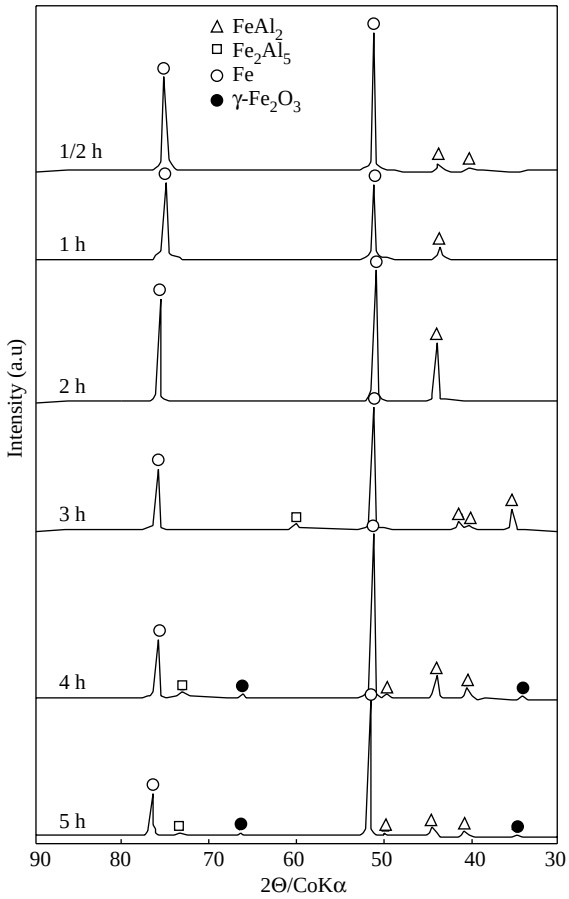

Figure 1. X-ray diffractograms of Al films of an initial thickness of 3 μm, which were grown on steel substrates and annealed for 30 min, 1 h, 2 h, 3 h, 4 h, and 5 h at 500 °C.

Table 1. The intermetallic phases observed by annealing of Fe-Al films at different temperatures, times, and initial thicknesses using XRD and EDS analysis.

		Initial Film Thickness			
Temperature T	Time t	2 μm	3 μm	8 μm	14 μm
300 °C	½ h	Fe_2Al_3			
	5 h		$FeAl_2$		
	1 h			$FeAl_3$	
500 °C	1/6 h	$FeAl_2$ Fe_2Al_5			
	½ h	$FeAl_2$ Fe_2Al_5	$FeAl_2$	$FeAl_2$	
	1 h	$FeAl_2$ Fe_2Al_5	$FeAl_2$	$FeAl_2$	
	2 h		$FeAl_2$	$FeAl_2$	
	3 h		$FeAl_2$ Fe_2Al_5	$FeAl_2$ Fe_2Al_5	$FeAl_2$
	4 h	$FeAl_2$ Fe_2Al_5 Fe_2O_3	$FeAl_2$ Fe_2Al_5 Fe_2O_3	$FeAl_2$ Fe_2Al_5 Fe_2O_3	$FeAl_2$
	5 h		$FeAl_2$ Fe_2Al_5 Fe_2O_3	$FeAl_2$ Fe_2Al_5 Fe_2O_3	$FeAl_2$
	8 h				$FeAl_2$
550 °C	4 h			$FeAl_2$	
650 °C	½ h		Fe_2Al_5 $FeAl_3$		

Table 2. The results of recent studies of the Fe-Al system.

Reference	Processing Method	Annealing Temperature	Intermetallics Detected
Chung and Chung (2006)	Computer Simulation	-	FeAl
Jindal et al. (2006)	Solid State Diffusion Couple	500 °C	Fe_2Al_5
Murakami et al. (2004)	Powder Liquid Aluminization	-	FeAl
Murakami et al. (2004)	Powder Liquid Aluminization	700-800 °C	$FeAl_2$-FeAl
Mengucci et al. (2003)	Electron Beam Evaporation	100-300 °C	$FeAl_2$-$FeAl_3$
Levin et al. (2001)	Crossed-Beam Pulsed Laser Deposition	50-950 °C	Fe_2Al_5
Levin et al. (2001)	Direct Pulsed Laser Deposition	50-950 °C	Fe_3Al-FeAl-Fe_2Al_5-$FeAl_2$
Carbucicchio et al. (1999)	Electron Beam Evaporation	-	$FeAl_2$-FeAl

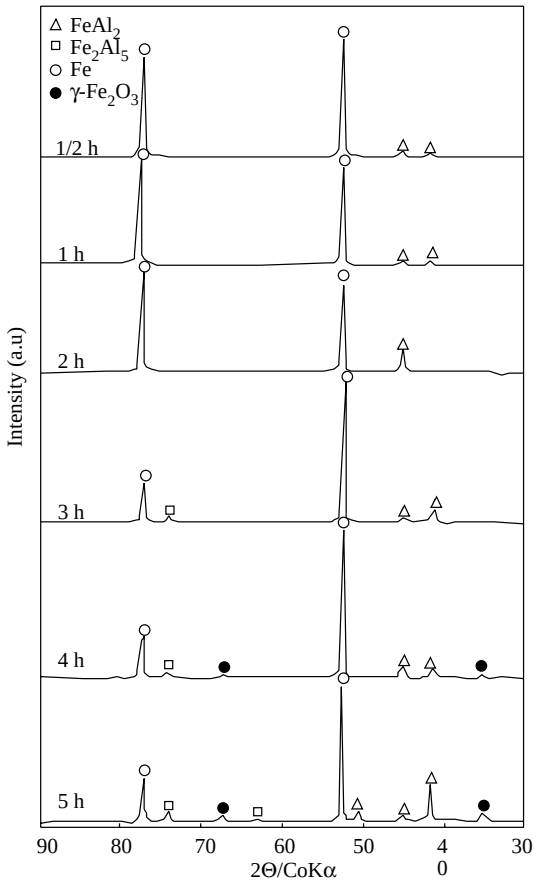

Figure 2. X-ray diffractograms of Al films of an initial thickness of 8 μm, which were grown on steel substrates and annealed for 30 min, 1 h, 2 h, 3 h, 4 h, and 5 h at 500 °C.

From these figures it could be concluded that at early stages of annealing the intermetallic phase $FeAl_2$, owing to its relatively low concentration of Al with respect to Fe_2Al_5, was detected. With a longer annealing time, Fe_2Al_5 was also observed, owing to a higher Al concentration. The formation sequence of these phases can be related to the 2-layer model of reactive diffusion for thin films and semi-infinite diffusion couples, according to the study by Philibert (1990), in which a compound is first formed and consequently a second one is favored through an appropriate time for diffusion supplied by the system. A similar behavior of sequential formation of interfacial intermetallic layers was also shown by Akdeniz and Mekhrabov (1998) in the case of Fe-based aluminide diffusion layers at the Fe-Al interface, in the presence of substitutional impurities. They analyzed the evolution of Fe-Al diffusion layers in terms of interfacial interaction potentials based on the statistical thermodynamic theory of multicomponent alloys combined with electronic theory in the pseudopotential approximation.

Generally, $FeAl_2$, which was the first phase observed, showed an increase in its intensity until 3 h of annealing, indicating that its amount was also increasing. However, with the start of the formation of the Fe_2Al_5 phase at 3 h of annealing time, the intensity of $FeAl_2$ began to decrease. This behavior can be explained by the fact that longer annealing times caused the depletion of the $FeAl_2$ phase in favor of the formation of the second phase Fe_2Al_5.

Although the annealing process was conducted under an argon atmosphere, the Fe_2O_3 phase was observed on the films with an initial thickness of 2μ, 3μ, and 8 μm, starting at 4 h of annealing. This behavior is attributed to the long annealing periods, which caused some amount of oxidation in the samples.

An SEM micrograph of the 8-μm thick aluminum film, which was grown on a steel substrate and annealed for 30 min at 500 °C, and an X-ray diffractogram of the same film on which the $FeAl_2$ intermetallic phase was detected are shown in Figures 3a and 3b, respectively. Similarly, in Figures 4a and 4b, an SEM micrograph of the 8-μm thick aluminum film, which was grown on a steel substrate and annealed for 3 h at 500 °C, and EDS analysis of the same film at points "1" and "2" showing the presence of the $FeAl_2$ and Fe_2Al_5 intermetallic phases are given, respectively.

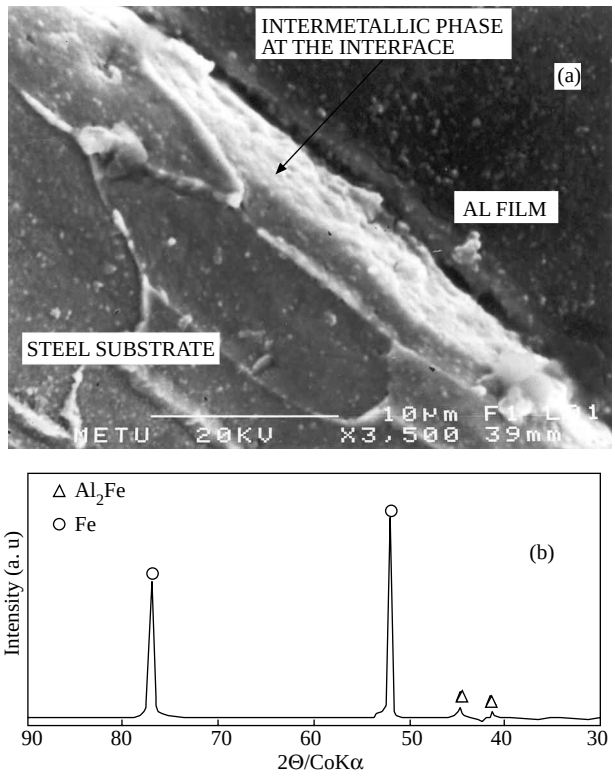

Figure 3a. SEM micrograph of 8-μm thick Al film, which was grown on a steel substrate and annealed for 30 min at 500 °C. **b.** X-ray diffractogram of the same film showing the presence of $FeAl_2$.

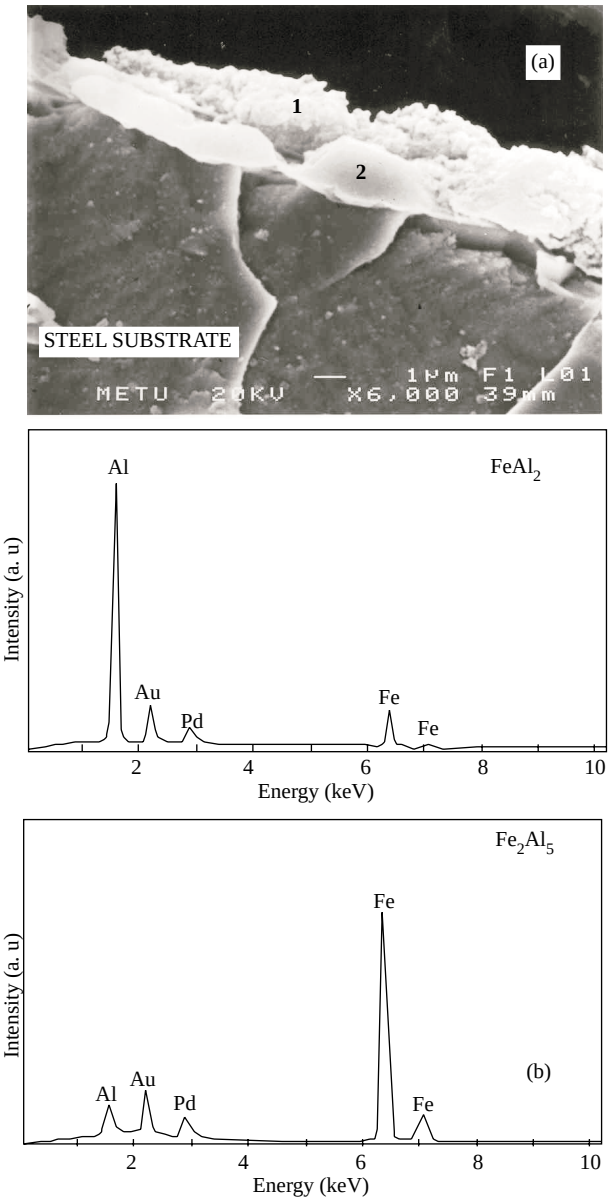

Figure 4a. SEM micrograph of the 8-μm thick Al film, which was grown on a steel substrate and annealed for 3 h at 500 °C. **b.** EDS spectra of the intermetallic phases at points "1" and point "2" showing the presence of $FeAl_2$ and Fe_2Al_5, respectively.

Annealing time and initial film thickness dependency of the intermetallics formed at the interfaces can be analyzed from these figures. As limited annealing time (30 min) was applied for the 8-μm thick Al film, only the $FeAl_2$ intermetallic phase was observed, whereas the 3-μm thick Al film annealed for a longer period (4 h) revealed 2 different intermetallic phases ($FeAl_2$ and Fe_2Al_5) due to the enhancement

of diffusion of Al into the steel substrate during this increased period of annealing.

Scanning Electron Microscopy (SEM) and Energy Dispersive Spectroscopy (EDS) analysis

The results of EDS analysis of the intermetallic phases observed by annealing at different temperatures are given in Table 3. Atomic percentages were converted to probable respective intermetallic phases with the help of their stability ranges. These results support and strengthen the XRD analysis of the same specimens, and are congruent with the recent studies presented in Table 2. $FeAl_2$, Fe_2Al_5, and $FeAl_3$ were commonly encountered intermetallics. $FeAl_2$ was the most dominant phase observed, mainly at higher initial film thickness values.

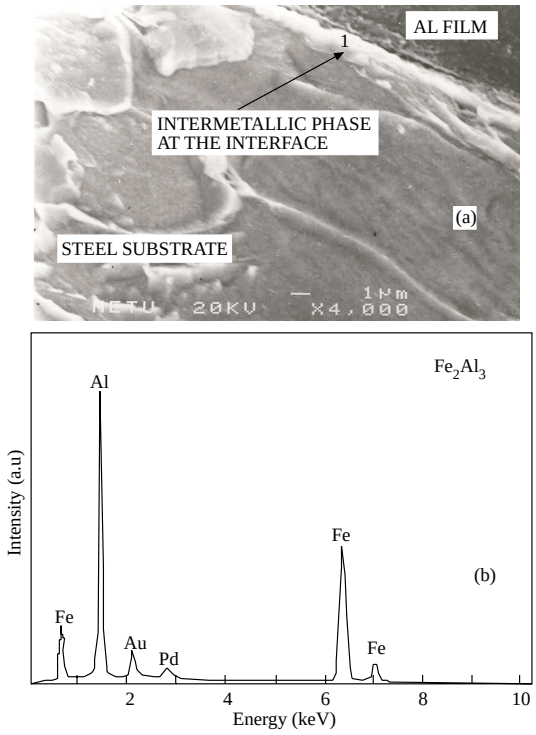

Figure 5a. SEM micrograph of the 2-μm thick Al film, which was grown on a steel substrate and annealed for 30 min at 300 °C. **b.** EDS spectrum of point "1" showing the presence of Fe_2Al_3 at the interface.

In Figures 5a and 5b, an SEM micrograph and EDS spectrum with general elemental distribution are shown, respectively, for the cross-section of the Al film with an initial thickness of 2 μm, which was grown on a steel substrate and annealed for 30 min at 300 °C. Similarly, the same type of SEM micrographs and EDS general elemental distribution results are shown at the same temperature of 300 °C for an initial thickness of 3 μm annealed for 5 h in Figures 6a and 6b, respectively. The last data reflected in an SEM micrograph and EDS analysis at 300 °C are shown in Figures 7a and 7b, for which the initial film thickness was 8 μm and the annealing period was 1 h. The intermetallic phases of Fe_2Al_3, $FeAl_2$, and $FeAl_3$ were observed at the above-mentioned experimental situations, respectively. It can be concluded that the atomic percentage Al of the intermetallic phases formed at the interfaces increased with initial Al film thickness. Fe_2Al_3 has atomic percentage Al between 58% and 65%. This intermetallic phase was observed at the initial film thickness of 2 μm, whereas atomic percentage Al of $FeAl_2$ was 66%-66.9%, which is a higher concentration when compared to Fe_2Al_3, and was observed at a higher initial film thickness (3 μm). Finally, at the highest initial film thickness of 8 μm, the highest atomic percentage Al was observed for $FeAl_3$ (74.5%-76.5%).

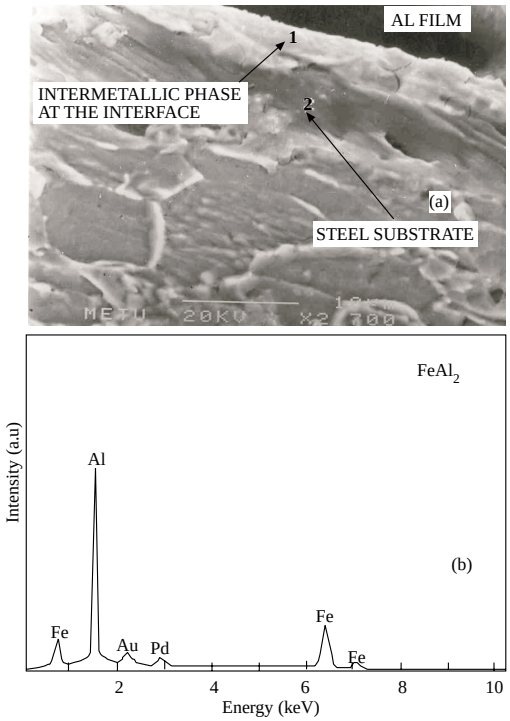

Figure 6a. SEM micrograph of the 3-μm thick Al film, which was grown on a steel substrate and annealed for 5 h at 300 °C. **b.** EDS spectrum of the same film at point "1" showing the presence of $FeAl_2$; point "2" denotes the steel substrate.

Table 3. The results of EDS analysis of the intermetallic phases observed by annealing at different temperatures. The numbers represent atomic percentages of the respective phases.

Initial Film Thickness	Heat Treatment Temperature-time	Phases Observed
2 μm	300 °C-30 min	(Fe: 38.61, Al: 61.39)→Fe_2Al_3
2 μm	500 °C-30 min	(Fe: 27.25, Al: 72.75)→ Fe_2Al_5(Fe: 33.96, Al: 66.04)→ $FeAl_2$
2 μm	500 °C-4 h	(Fe: 29.87, Al: 70.13)→ Fe_2Al_5
3 μm	300 °C-5 h	(Fe: 33.27, Al: 66.73)→ $FeAl_2$
3 μm	500 °C-30 min	(Fe: 34.36, Al: 65.64)→ $FeAl_2$
3 μm	500 °C-2 h	(Fe: 34.44, Al: 65.56)→ $FeAl_2$
3 μm	650 °C-30 min	(Fe: 28.51, Al: 71.49)→Fe_2Al_5 (Fe: 23.07, Al: 76.98)→ $FeAl_3$
8 μm	300 °C-1 h	(Fe: 24.57, Al: 75.43)→ $FeAl_3$
8 μm	500 °C-2 h	(Fe: 32.79, Al: 67.21)→ $FeAl_2$
8 μm	500 °C-3 h	(Fe: 33.68, Al: 66.32)→ $FeAl_2$
8 μm	500 °C-4 h	(Fe: 32.54, Al: 67.46)→ $FeAl_2$
8 μm	500 °C-5 h	(Fe: 36.02, Al: 63.98)→ $FeAl_2$
8 μm	550 °C-4 h	(Fe: 34.76, Al: 65.24)→ $FeAl_2$
14 μm	500 °C-3 h	(Fe: 33.27, Al: 66.73)→ $FeAl_2$
14 μm	500 °C-4 h	(Fe: 33.09, Al: 66.91)→ $FeAl_2$

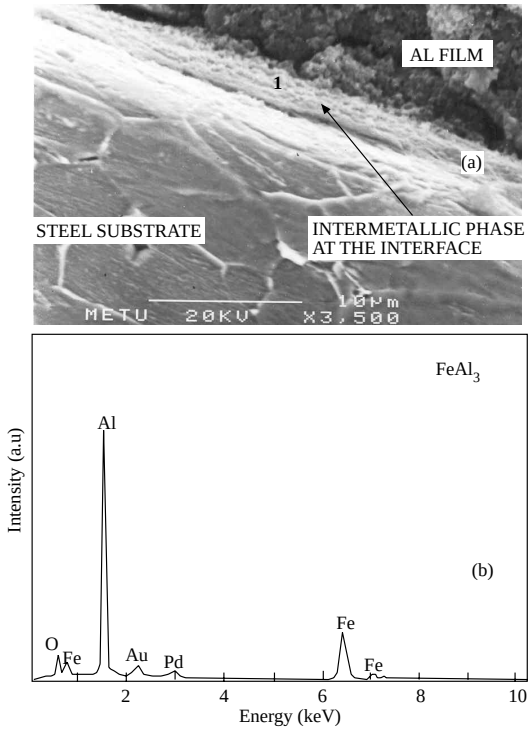

Figure 7a. SEM micrograph of the 8-μm thick Al film, which was grown on a steel substrate and annealed for 1 h at 300 °C. **b.** EDS spectrum of the same film at point "1" showing the presence of $FeAl_3$.

Conclusion

Intermetallic phase $FeAl_2$ appeared first at the Fe-Al film interface for most of the designed experimental conditions. This result was supported thermodynamically as it had the lowest free energy of formation in the Fe-Al system when compared to other intermetallics at the Al-rich region of the Fe-Al phase diagram.

Intermetallic phase Fe_2Al_5 was observed after the formation of intermetallic phase $FeAl_2$. Three conditions can be given for the formation of intermetallic phase Fe_2Al_5. It was achieved first with an increase in annealing time at constant temperature. Secondly, it was achieved with the decrease in initial film thickness at constant annealing temperature and annealing time. The last condition for the formation of intermetallic phase Fe_2Al_5 was by increasing the annealing temperature at constant initial Al film thickness, and at constant annealing time.

Atomic Al percentage of the intermetallic phase formed increased with initial Al film thickness, which was evidenced through all the experiments. All the phases present in the equilibrium diagram did not necessarily appear and they did not necessarily begin to grow simultaneously, but various incubation periods were observed. They were formed sequentially, in contrast to intermetallics, which formed synchronously in bulk materials.

References

Akdeniz, M.V. and Mekhrabov, A.O., "The Effect of Substitutional Impurities on the Evolution of Fe-Al Diffusion Layer", Acta Materialia, 46, 1185-1192, 1998.

Carbucicchio, M., Grazzi, C., Rateo, M., Ruggiero, G and Turilli, G., "Microstructure and Magnetic Properties of Iron-Aluminum Multilayers", Nanostructured Materials, 11, 775-782, 1999.

Chung, C.Y. and Chung, Y.C., "Molecular Dynamics Simulation of Nano-scale Fe-Al Thin Film Growth", Materials Letters, 60, 1063-1067, 2006.

Güler, H., "Formation of Intermetallic Phases at the Metal-Silicon Interfaces", PhD Thesis, METU, Ankara, 2001.

Jindal, V., Srivastava, V.C., Das, A. and Ghosh, R.N., "Reactive Diffusion in the Roll Bonded Iron-aluminum System", Materials Letters, 60, 1758-1761, 2006.

Levin, A.A., Meyer, D.C., Paufler, P., Gorbunov, A., Tselev, A. and Gawlitza, P., "Thermally Stimulated Solid State Reactions in Fe-Al Multilayers Prepared by Pulsed Laser Deposition", Journal of Alloys and Compounds, 320, 114-125, 2001.

Mengucci, P., Majni, G., Di Cristoforo, A., Checchetto, R., Miotello, A., Tosello, C. and Principia, G., "Structural Evolution of Fe-Al Multilayers Submitted to Thermal Annealing", Thin Solid Films, 433, 205-210, 2003.

Murakami, K., Nori, N., Osamura, K. and Tomota, Y., "Aluminization of High Purity Iron by Powder Liquid Coating", Acta Materialia, 52, 1271-1281, 2004.

Özenbaş, M. and Güler, H., "Formation of Al-Si Intermetallic Phases", Chem. Eng. Comm., 190, 911-924, 2003.

Philibert, J., "Reactive Diffusion", Defect and Diffusion Forum 66-69, 995, 1990.

Wang, Z., Zhou, Y. and Xia, Y., "Effect of Strain Rate on Behavior of Fe_3Al under Tensile Strength", J. Materials Science, 32, 2387, 1997.